

# Liquid, Glass and Crystal in Two-dimensional Hard disks

Ludger Santen and Werner Krauth \*

*CNRS-Laboratoire de Physique Statistique*

*Ecole Normale Supérieure, 24, rue Lhomond, 75231 Paris Cedex 05, France*

We study the thermodynamic and dynamic phase transitions in two-dimensional polydisperse hard disks using Monte Carlo methods. A conventional local Monte Carlo algorithm allows us to observe a dynamic liquid-glass transition at a density  $\rho^G$ , which depends very little on the degree of polydispersity. We furthermore apply Monte Carlo methods which sample the Boltzmann equilibrium distribution at any value of the density and polydispersity, and remain ergodic even far within the glass. We find that the dynamical transition at  $\rho^G$  is not accompanied by a thermodynamic transition in this two-dimensional system so that the glass is thermodynamically identical to the liquid. Moreover, we scrutinize the polydispersity-driven transition from the crystal into the disordered phase (liquid or glass). Our results indicate the presence of a continuous (Kosterlitz-Thouless type) transition upon increase of the polydispersity.

For several decades now, enormous interest has been concentrated on the glass transition in classical liquids [1]. At this transition, the viscosity of a structurally disordered liquid increases dramatically and reaches values typical of a crystalline solid. The underlying reasons for the spectacular slowdown of the system's time evolution have been hotly debated and views very much diverge on this question [2–5]. The transition is naturally related to the loss of thermal equilibrium during the quench towards low temperatures, and it is well-known that the properties of a glass strongly depend on the detailed quench procedure [6]. The theoretical description of this phenomenon in all its complexity is a very difficult task.

Notwithstanding the intimate relationship of the glass transition with *loss* of thermal equilibrium (*i.e.* ergodicity breaking), it is nevertheless possible to describe the glass *within* thermal equilibrium. This means that one studies configurations of the system taken from the Boltzmann distribution (which exists in a mathematical sense at any temperature and pressure) and computes their thermodynamic and dynamic properties. For any thermodynamically stable glass, the reference to the quench history can thus be omitted, and the theoretical analysis is much simpler.

The most serious problem with the ‘equilibrium glass’ is of course that the Boltzmann distribution is experimentally inaccessible inside the glassy phase. Attempts to characterize the true equilibrium properties of a glass necessarily rely on the extrapolation of experimental data.

However, computational methods have been developed which allow to bypass this obstacle: non-local Monte Carlo (MC) algorithms *can* remain ergodic in the glassy phase for prominent model systems, such as hard spheres, and allow to compute their equilibrium observables directly [7]. With this approach, we may address questions

at the heart of long-standing controversies, for example about the existence of an inaccessible thermodynamic phase transition within the glass, which has been rendered responsible for the dynamic transition [2–5].

In the past, many classical statistical physics models have been considered in the study of glasses. For a long time, it was believed that the very simplest model systems (monodisperse hard spheres, hard disks, and central potential models) did also possess a glassy phase [8]. However, more recent MC simulations have shown that monodisperse hard spheres always crystallize, and that the previously observed behavior was mainly due to finite-size effects and limited computer resources [9]. This has also been confirmed in experiments with colloidal systems, where crystallization preempts the glass transition for monodisperse hard spheres. In order to avoid parasitic effects, some of the experiments have been performed in zero-gravity environments [10].

The situation changes abruptly, both in experiment [11] and in the simulations, in the presence of a small dispersity in size. Several investigations have shown the existence of a so-called ‘terminal polydispersity’ of a few percent (*cf. e.g.*, [12,13]), above which crystallization can be avoided for any value of the external pressure, *i.e.*, up to very high densities.

Polydispersity opens up opportunities to study two very interesting, yet distinct phenomena: (*i*) the glass transition, which is no longer preempted by crystallization at sizeable values of the polydispersity; (*ii*) the thermodynamic transition of the crystal into a disordered state (liquid or glass) upon an increase of the polydispersity.

In the present work, we study these two phenomena in two-dimensional hard disks. We investigate their dynamical and thermodynamical phase diagram as a function of density  $\rho$  (or pressure  $P$ ) and of the polydispersity for a

---

\*santen@lps.ens.fr; krauth@lps.ens.fr, <http://www.lps.ens.fr/~krauth>

given functional form of the size dispersion. At polydispersities for which crystallization is impossible, we find a purely dynamic liquid-glass transition at a density  $\rho^G$ , which depends very little on the degree of polydispersity  $\varepsilon$ . For moderate values of  $\varepsilon$ , the glass transition density can be defined even better than in the highly polydisperse case considered earlier [7]. Interestingly,  $\rho^G$  is considerably higher than the crystallization density for the monodisperse system.

Our vastly improved equilibrium simulation methods allow us to scan the complete parameter space  $(\varepsilon, \rho)$ . Even far inside the glassy phase, we can compute the equation of state and the compressibility with very high precision. The polydispersity-driven transition of the crystal into the disordered phase (liquid or glass) also turns out to be particularly interesting: we find strong evidence that this disorder-driven phase transition is continuous. Our findings can hardly be reconciled with the presence of a first-order transition, and differ from what was stated in a closely related work [14].

In principle, for a polydisperse mixture of particles, one should choose the particle sizes  $r_i$  independently from a given probability distribution  $p(r)$ . We would then have to perform an ensemble average over the distribution of radii. In dynamical simulations, this average corresponds to ensemble-averaging time correlation functions of a given sample. In thermodynamic calculations, the average over radii can be incorporated directly into the MC evaluation of the partition function, as some authors have done [12].

We have adapted a much simpler, yet practically equivalent approach, by considering a ‘fixed probability increment’ model for any probability distribution  $p(r)$  with  $r > 0$ , where we pick the  $N$  radii  $r_i$  *e.g.* according to the following equation

$$\int_0^{r_i} dr p(r) = \frac{i}{N+1} \quad (1)$$

(with  $\int_0^\infty dr p(r) = 1$ ). In this way, sample-to-sample fluctuations are completely eliminated, and the most representative sample is generated for an arbitrary distribution  $p(r)$ .

Here, we study a model with a flat distribution of radii:

$$p(r) = \begin{cases} \text{const} & r_{min} \leq r \leq r_{max} \\ 0 & \text{otherwise,} \end{cases} \quad (2)$$

*i.e.* the radii are given by  $r_i = r_1 + \Delta(i-1)$  (with  $\Delta = (r_n - r_1)/(N-1)$ ). As in [15], we set the total particle volume as  $V_{part} = N\pi/4$  and the Boltzmann factor as  $\beta = 1$ .

We define the polydispersity by the normalized width of the distribution eq.(2)

$$\varepsilon = \sqrt{\langle \delta r^2 \rangle} / \langle r \rangle^2. \quad (3)$$

Notice that the distribution eq.(2) satisfies  $\varepsilon \leq 1/\sqrt{3}$ , this limit being attained for  $r_{min} = 0$ .

Our simulations are performed in a periodic box of size  $L \times \sqrt{3}L/2$ , as is customary [15], and the only difference in set-up between our thermodynamic and dynamic simulations is the choice of ensembles. The equation of state  $V(P)$  is most naturally computed in the [NP] ensemble, where the size of the box is allowed to fluctuate. The dynamical calculations are done in the [NV] ensemble, where the time evolution of states can be best monitored. For these calculations, a conventional local MC algorithm is used. Up to a trivial rescaling of time, we expect this algorithm in the long-time limit to give the same results as a molecular dynamics method.

The equilibration of polydisperse systems is a difficult task, because the properties of the system depend sensitively on the relative arrangements of particles, which have to be averaged over. Therefore, one needs an algorithm that moves particles over large distances and averages over different possible arrangements. In the fluid phase this can in principle be achieved by a long series of local moves. In the crystal or the glass, it is however mandatory to equilibrate the system by non-local moves, as in the pivot cluster algorithm [16].

A polydisperse system with a continuous distribution of radii is easier to simulate than a binary distribution, because it is often possible to exchange particles with similar radii. These swaps also implement non-trivial long-range moves, and have to be combined with a local Monte Carlo algorithm. The acceptance probability for such swaps decreases only at the most extreme densities, when each particle is so close to its neighbors that it can virtually never be replaced by a particle with slightly larger radius.

In high-density *binary* mixtures (*cf* [17]), the pivot cluster algorithm is clearly more appropriate, because the direct particle exchanges freeze out. In the present *polydisperse* case, however, we have obtained identical results with both algorithms for systems of  $N = 256$  and  $N = 1024$  particles even slightly below what we believe to be close packing.

Extensive tests of ergodicity (*cf* [7]) fully confirm the above statements: In very small systems ( $N = 15$ ), where the minimal size differences between particles are larger, we can show that the direct swap algorithm falls out of equilibrium at slightly *lower* densities than the pivot cluster method for the above-mentioned reasons.

We point out a completely unrelated, yet crucial, issue: To compute the equation of state at constant pressure, we need to include volume changes into the MC algorithm. Extremely time-consuming sampling of the volume by trial and error (using the Metropolis algorithm [15]) can be avoided [12,18,20].

For orientation, we show in figure 1 the schematic phase diagram as a function of density  $\rho$  and polydispersity  $\varepsilon$  (*cf* eq.(3)) which results from our thermodynamic

and dynamic calculation, and which we discuss in the remainder of this paper. We have studied this diagram by the routes indicated by gray lines in the figure, using either the non-local MC algorithm (for thermodynamic averages), or the local MC method (to study the dynamics).

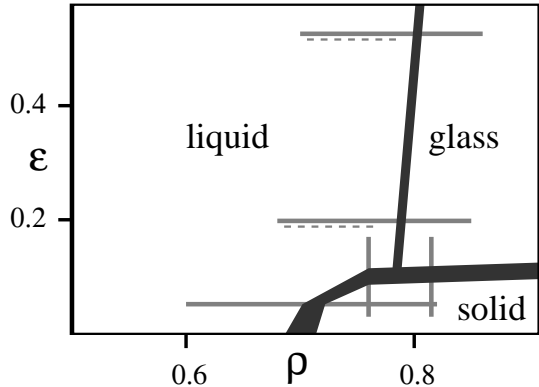


FIG. 1. Schematic phase diagram of the two-dimensional hard-disk system as function of polydispersity  $\varepsilon$  and density  $\rho$ . The dark lines indicate estimated phase boundary (obtained by linear interpolation of data points). The gray lines correspond to the paths along which calculations were performed. Full lines: thermodynamic calculations (non-local MC algorithm); broken lines: dynamic calculations (local MC).

In Figure 2a, we show the liquid and solid branches of the thermodynamic equation of state as a function of pressure  $P$  for a fixed  $\varepsilon = 0.052$ . The presence of a thermodynamic transition is evident.

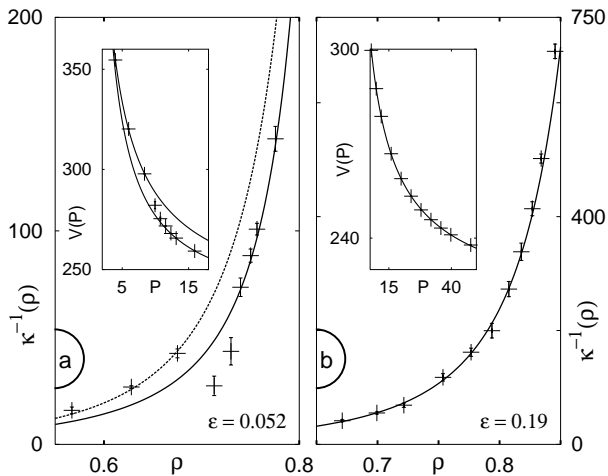


FIG. 2. Inverse compressibility  $\kappa^{-1}$  as a function of density  $\rho$  and equation of state  $V(P)$  for two values of the polydispersity  $\varepsilon$  at  $N = 256$ . Left:  $\varepsilon = 0.052$ : a thermodynamic phase transition is clearly detectable, both in  $V(P)$  and in  $\kappa^{-1}$ . Right:  $\varepsilon = 0.19$ : No thermodynamic phase transition can be detected.  $\kappa$  is obtained by derivation of the curve  $V(P)$  and by direct computation from the fluctuations of the volume.

In these calculations at  $\varepsilon = 0.052$ , and at  $N = 256$ , we are able to establish coexistence of the two phases as in the monodisperse system [15]. Even there however, the  $N \rightarrow \infty$  limit has remained controversial, and it is not yet firmly established whether the liquid-solid transition in 2-d monodisperse disks is first-order or continuous (according to the KTNHY scenario, *cf* [21]). Notice that the transition shows up very clearly both in the equation of state and in the compressibility, shown in the main figure 2a.

In figure 2b, we show analogous data for  $\varepsilon = 0.19$ . There, we see no indication of a thermodynamic phase transition in the whole range of densities studied. Similar results were obtained at  $\varepsilon = 0.52$  (remember that  $\varepsilon < 0.58$  *cf* text following eq.(3)); these data confirm and considerably extend our earlier calculations [7]. Within our flat probability distribution of the radii of particles, there exists a maximal polydispersity  $\varepsilon = 0.58$ , which corresponds to the limit  $r_{min} \rightarrow 0$  in eq.(2).

Our calculations thus confirm the existence of a terminal polydispersity, which was studied mostly in three dimensions, but also evoked in related two-dimensional work [14].

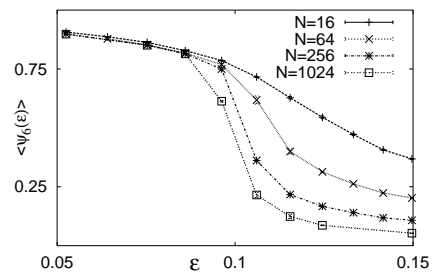


FIG. 3. Average bond-orientational order-parameter for  $P = 17.1$ . For polydispersities  $\varepsilon \leq 0.08$ , the measurements converge towards a size-independent value, while we expect  $\langle \Psi_6 \rangle \rightarrow 0$  for larger polydispersities. The probability distributions of  $\Psi_6$  are unimodal, and give no indication of a first-order phase transition. Notice the smoothness of the finite-size behavior, which is due to our choice of the fixed-probability increment model eq.(1).

The horizontal sweeps in the phase diagram of figure 1 bracket the disordered-to-crystalline phase boundary, which must be essentially independent of  $\varepsilon$  at large  $\rho$ . We further studied the thermodynamic system as a function of polydispersity at constant pressure, along the vertical paths indicated in figure 1. There, our data strongly favor a continuous transition: We did not find hysteresis in  $V(P)$ , and detected no abrupt change of the volume distribution function in the transition region. We also computed the average bond-orientational order-parameter  $\langle \Psi_6 \rangle$  (*cf*, *e.g.*, [22] for definitions and a discussion). There also, the probability distribution of  $\Psi_6$  has a single peak, and is perfectly reproduced, without any indications of hysteresis. We conclude that the

transition is continuous. In figure 3 we show  $\langle \Psi_6 \rangle$  as a function of polydispersity  $\varepsilon$  for different system sizes. A detailed, more rigorous study of the probable two-step melting process in this system is left for further work. Let us note that the numerical analysis of the standard Kosterlitz-Thouless transition has proven to be very subtle even in the prototypical XY-model [23].

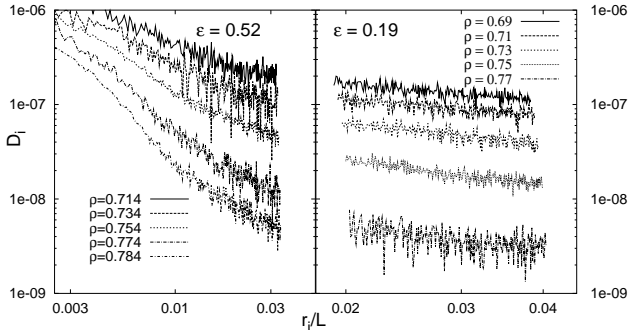


FIG. 4. Long-time diffusion constants as a function of particle size  $r_i/L$  for two values of the polydispersity  $\varepsilon$ . Left:  $\varepsilon = 0.52$ , right:  $\varepsilon = 0.19$ . In both cases, we witness a dramatic slow-down of the time-evolution as the density  $\rho^G \simeq 0.8$  is approached. This density is much higher than the liquid-solid transition density of the monodisperse hard-disk system, but much smaller than the densities which we can reach (within thermal equilibrium) with the non-local algorithms.

Finally, we determine the dynamic properties of the system, in the [NV] ensemble, with the local MC algorithm, and at values of  $\varepsilon$  which ensure the absence of a liquid-solid transition. Using the protocol of ref. [7], we obtained the effective diffusion constants  $D_i$  (cf figure 4), for  $\varepsilon = 0.19$  and  $\varepsilon = 0.52$ . In both cases, the results are consistent with the scaling form [24]:

$$D_i(\rho) \sim (\rho_i^G - \rho)^\alpha, \quad (4)$$

where we extrapolate the diffusion constants for each particle separately. The diffusion constants  $D_i$  strongly depend on  $i$ , but the extrapolated transition densities  $\rho_i^G$  do not, especially for small  $\varepsilon$ . We take these extrapolated values as a definition of the glass transition density  $\rho^G$ . Only at large  $\varepsilon$  (left part of figure) can some very small particles ( $r_{min}/r_{max} = 19$ ) escape through slits left open in the system. This leads to some additional structure in the  $D_i$  plot on the left half of figure 4, and to an increased value of the extrapolated  $\rho_i^G$  for small  $i$ .

In conclusion, our study of the polydisperse hard disk system has given the homogeneous phases shown in the schematic diagram figure 1. Inhomogeneous phases [13] seem to play no role at the parameters studied in this paper. A tendency towards phase separation should first show up in irregular finite-size behavior, which we have not encountered. We find it particularly significant that the glass transition depends so little on polydispersity, and takes place at densities (and pressures) much higher

than the crystallization density in the monodisperse system. Using our specialized MC methods, we are able to probe the thermodynamics of the hard-disk system far within the glassy phase, where we find no indications of an accompanying thermodynamic transition.

Acknowledgements: We thank P. Le Doussal for helpful discussions. L. S. acknowledges support from the Deutsche Forschungsgemeinschaft under Grant No. SA864/1-2.

- 
- [1] For a recent overview see the articles in: *Science* **267**, Iss. 5206 (1995); *J. Phys.: Cond. Mat.* **11**, Iss. 10A (1999).
  - [2] W. Kauzmann, *Chem. Rev.* **43**, 219 (1948).
  - [3] J. H. Gibbs, E. A. DiMarzio, *J. Chem. Phys.* **28**, 373 (1958).
  - [4] M. Mezard, G. Parisi, *Phys. Rev. Lett.* **82**, 747 (1999).
  - [5] N. Menon, S. R. Nagel, *Phys. Rev. Lett.* **74**, 1230 (1995).
  - [6] K. Vollmayr, W. Kob, K. Binder, *Europhys. Lett.* **32**, 715 (1995).
  - [7] L. Santen, W. Krauth, *Nature* **405**, 550 (2000).
  - [8] L. V. Woodcock, *Ann. (N. Y.) Acad. Sci.* **37**, 274 (1981).
  - [9] M. D. Rintoul, S. Torquato, *Phys. Rev. Lett.* **77**, 4198 (1996).
  - [10] W. B. Russel, P. M. Chaikin, J. Zhu, W. V. Meyer, R. Rogers, *Langmuir* **13**, 3871 (1997).
  - [11] W. van Meegen, T. C. Mortensen, S. R. Williams, J. Müller, *Phys. Rev. E* **58**, 6073 (1998).
  - [12] D. A. Kofke, P. G. Bolhuis, *Phys. Rev. E* **59**, 618 (1999).
  - [13] P. Bartlett, *J. Chem. Phys.* **109**, 10970 (1998).
  - [14] M. R. Sadr-Lahijany, P. Ray, H. E. Stanley, *Phys. Rev. Lett.* **79**, 3206 (1996); *Physica A* **270**, 295 (1999).
  - [15] J. Lee, K. J. Strandburg, *Phys. Rev. B* **46**, 11 190 (1992).
  - [16] C. Dress, W. Krauth, *J. Phys. A: Math. Gen.* **28**, L597 (1995).
  - [17] T. S. Grigera, G. Parisi, *Phys. Rev. E* **63**, 045102 (2001).
  - [18] L. Santen, W. Krauth (in preparation).
  - [19] W. H. Press, S. A. Teukolsky, W. T. Vetterling, B. P. Flannery, *Numerical Recipes in C*, (2nd ed. Cambridge University Press, 1998).
  - [20] A volume-step consists in calculating the *minimal* accessible box volume  $V_{min}$  upon rescaling of the present configuration, and in randomly choosing the *actual* box volume  $V$ . The correct probability to choose  $V$  is given by  $p(V) \propto V^N \exp(-PV)$ , for  $V \geq V_{min}$ .  $p(V)$  can be sampled exactly, as any one-dimensional distribution [19]. In our case, at high pressure  $P$ , we approximate  $p(V)$  without loss of accuracy as  $p(V) = \lambda \exp(-\lambda(V - V_{min}))$ , where  $\lambda = P - N/V_{min}$ .
  - [21] K.J. Strandburg, *Rev. Mod. Phys.* **60**, 161 (1988).
  - [22] H. Weber, D. Marx, K. Binder, *Phys. Rev. B* **51**, 14636 (1995).
  - [23] P. Olsson, *Phys. Rev. B* **52**, 4511 (1995); *Phys. Rev. B* **52**, 4526 (1995).
  - [24] M. Fuchs, W. Götze, M. R. Mayr, *Phys. Rev. E* **58**, 3384 (1998).